

Energy Transfer in Multi Field Inflation and Cosmological Perturbations

Amjad Ashoorioon^{◆1}, Axel Krause^{♣2} and Krzysztof Turzynski^{◆♠3}

*◆Michigan Center for Theoretical Physics
University of Michigan, Ann Arbor
Michigan 48109-1040, USA*

*♣Arnold Sommerfeld Center for Theoretical Physics
Department für Physik, Ludwig-Maximilians-Universität München,
Theresienstr. 37, 80333 Munich, Germany*

*♠Institute of Theoretical Physics
University of Warsaw,
ul. Hoża 69, 00-681 Warsaw, Poland*

Abstract

In cascade inflation and some other string inflation models, collisions of mobile branes with other branes or orbifold planes occur and lead to interesting cosmological signatures. The fundamental M/string-theory description of these collisions is still lacking but it is clear that the inflaton loses part of its energy to some form of brane matter, e.g. a component of tensionless strings. In the absence of a fundamental description, we assume a general barotropic fluid on the brane, which absorbs part of the inflaton's energy. The fluid is modeled by a scalar with a suitable exponential potential to arrive at a full-fledged field theory model. We study numerically the impact of the energy transfer from the inflaton to the scalar on curvature and isocurvature perturbations and demonstrate explicitly that the curvature power spectrum gets modulated by oscillations which damp away toward smaller scales. Even though, the contribution of isocurvature perturbations decays toward the end of inflation, they induce curvature perturbations on scales that exit the horizon before the collision. We consider cases where the scalar behaves like radiation, matter or a web of cosmic strings and discuss the differences in the resulting power spectra.

¹amjad@umich.edu

²axel.krause@physik.uni-muenchen.de

³turzyn@fuw.edu.pl

1 Introduction

There has been a lot of activity over the past few years to derive inflation from string theory. Most prominent among the many approaches has been brane inflation, in which the coordinates of some mobile branes on the internal compactification manifold provide the inflatons in the effective four-dimensional low energy theory [1]. While initial efforts focussed, for simplicity, on compactifications with a single mobile brane (for recent updates on single brane inflations, see e.g. [2]-[10]) general compactifications with fluxes naturally possess several, often many, mobile branes to satisfy tadpole cancellation equations [11]-[16]. Multi brane inflation models lead to multi field inflation cosmologies in the low energy theory, which as a result have been actively researched recently (see e.g. [17]-[39]). The multitude of inflaton fields can be actually seen as a physical blessing rather than a technical curse.

The multi brane inflation models split into two classes: those with brane-brane interactions which steer the multi brane system towards a stable dynamical attractor and those with brane-brane interactions for which no such attractor exists. The first class allows to replace the multi field cosmologies by cosmologies involving fewer fields, in the extreme case just a single inflaton field, once the system evolves along the attractor. An example for the first class is a multi brane system with exponential interactions among the branes, caused by non-perturbative interactions between classically non-interacting branes [11]. As a result of the stable attractor evolution this class more readily allows for an analytical treatment and moreover offers a parametric way to achieve inflation. Namely by choosing the number of participating branes large enough, one achieves a parametric suppression of the slow-roll parameters – a phenomenon which is known as assisted inflation [40].

The second class, on the other hand, requires an enormous fine-tuning for the position of each mobile brane in order to yield an ordered, e.g. equidistant, brane configuration, which admits an analytical treatment. An example of this class would be a system consisting of many brane-antibrane pairs with mutual Coulomb interactions. Full-fledged numerical studies for the cosmic evolution of this second class still need to be performed. Nevertheless, one might expect that this second class won't lead to inflation. The reason is that even if one starts with a multi brane configuration suitable for inflation (which, as said, requires a tremendous fine-tuning for all brane positions as the system lacks an attractor), small perturbations won't die away. They will lead the system to a complicated multi brane dynamics which moves the branes around on the internal space in an unconcerted way, precluding the realization of assisted inflation. The upshot might be that among the many

possible multi brane models, the models of the first class are the ones capable of generating inflation, whereas the models of the second class have to be dismissed.

In this paper we focus on a new phenomenon which arises in multi brane inflation models: the possibility of cascade inflation phases [13]. These arise when some of the mobile branes collide successively with fixed branes or orbifold fixed planes and thus no longer participate in the inflation process. The parameters of the effective four-dimensional inflationary potential vary in these collisions and as a result the inflationary potential acquires features. A characteristic consequence of such features is a damped oscillatory behavior of the power spectrum of density perturbations. This could lead to important observational clues about the underlying time variation of the inflationary potential.

To date, we have no complete fundamental M/string-theory description of such collisions. Therefore, we have to model the collision in field theory as an energy transfer (ET) from the inflaton to the brane. For instance, the brane could be modeled by a perfect fluid with a coupling to the inflaton which allows to transfer the inflaton's energy in discrete steps. More adapt to a field theory description based on a Lagrangean, and the route we follow here, is to model the perfect fluid by a scalar field with appropriate potential. Our goal in this paper is to study the potentially observable imprints of this ET on the resulting curvature and isocurvature perturbation spectrum. Chapter 2 describes the M-theory motivation and background for our analysis, reviewing cascade inflation. Chapter 3 introduces our two scalar field theory, which models the ET in brane collisions such as arising in cascade inflation. Chapter 4 presents the curvature and isocurvature perturbations for this model. We find that the contribution of isocurvature perturbations decays toward the end of inflation. Nonetheless, they induce curvature perturbations on scales that exit the horizon before the collision. The curvature power spectrum gets modulated by oscillations which damp away toward smaller scales. Finally, technical details on how to calculate the perturbations in our two-field model are presented in the Appendix.

2 Cascade Inflation

The goal of this paper is to study perturbations generated in a two scalar field inflation model with exponential potentials. Such potentials arise in fundamental physics from M-theory multi brane inflation [11] and cascade inflation [13] through non-perturbative instanton interactions. Since the two scalar field inflation model might also be used to provide some first insight into the cosmological impact of the ET arising when a bulk M5-brane collides with

the boundary in cascade inflation, we will now briefly recall cascade inflation as one of the motivations for our study.

Cascade inflation arises from heterotic M-theory [47], [48] compactified on $\mathbf{X} \times \mathbf{S}^1/\mathbf{Z}_2$, where \mathbf{X} is a Calabi-Yau threefold. Tadpole cancellation requires generically the presences of N M5-branes in the background. These fill the four-dimensional spacetime and wrap a holomorphic two-cycle on \mathbf{X} of genus zero. As BPS objects, the M5-branes interact only non-perturbatively via open M2-instantons which stretch along $\mathbf{S}^1/\mathbf{Z}_2$ and wrap the same two-cycle¹. The effective four-dimensional $\mathcal{N} = 1$ supergravity resulting from this compactification contains as scalar components of complex chiral superfields the M5-brane position moduli Y_i , $i = 1, \dots, N$, the Calabi-Yau \mathbf{X} volume modulus S and the $\mathbf{S}^1/\mathbf{Z}_2$ orbifold-size modulus T . Twice their real parts are denoted by y_i , s and t . Moreover, it's convenient to define $y = (\sum_{i=1}^N y_i^2)^{1/2}$. One can show that the M-theory dynamics leads to an equidistant distribution of the M5-branes along $\mathbf{S}^1/\mathbf{Z}_2$ [11]. For such a distribution

$$\text{Re}(Y_{i+1} - Y_i) \equiv \left(\frac{t}{2L}\right)\Delta x \quad (1)$$

is independent of the M5-brane counting label i . Consequently, the $N - 1$ inflatons $\text{Re}(Y_{i+1} - Y_i)$ can be identified. The multi inflaton system reduces effectively to one with a single inflaton Δx . The $\mathbf{S}^1/\mathbf{Z}_2$ interval size is denoted by L .

In the large volume limit, specified by the inequality $st \gg y^2$, where supergravity provides a reliable description of the dynamics [11], the potential for the canonically normalized inflaton $\varphi \sim N^{3/2}\Delta x$ becomes

$$V_N(\varphi) = V_N e^{-\sqrt{\frac{2}{p_N}} \frac{\varphi}{M_{\text{P}}}}, \quad (2)$$

where

$$V_N = (N - 1)^2 \left(\frac{6M_{\text{P}}^4}{st^3 d}\right), \quad p_N = \frac{4N(N^2 - 1)}{3st} \quad (3)$$

and d is the Calabi-Yau intersection number. For the detailed derivation from M-theory we refer the reader to [11, 13]. The cosmological FRW evolution in this background is given by power law inflation [49] with FRW scale factor

$$a(t) = a_0 t^{p_N}. \quad (4)$$

Inflation sets in when $p_N > 1$, which can always be achieved when sufficiently many M5-branes are present since $p_N \sim N^3$. Besides this bound on N from below, there is also a

¹For simplicity we are assuming a Calabi-Yau threefold with Hodge number $h^{(1,1)}(\mathbf{X}) = 1$.

bound on N from above which follows from the requirement to work in the large volume regime where $st \gg y^2$ holds and the fact that y grows with N . For typical parameter values one thus finds $20 \leq N \leq 200$ as a constraint on the number of M5-branes [11]. Such numbers can easily be accounted for in heterotic M-theory flux compactifications [50, 51, 52] where tadpole cancellation equations balance the amount of M5-branes with quantized flux numbers.

The repulsive M2-instanton interactions between the M5-branes cause them to spread over the $\mathbf{S}^1/\mathbf{Z}_2$ interval until the two outermost M5-branes hit the boundaries and dissolve into them via small instanton transitions [53], [54], [55]. This process changes the topological data on the boundaries while the number of M5-branes participating in the inflationary bulk dynamics drops from N to $N - 2$. The remaining $N - 2$ bulk M5-branes will continue to spread until again the most outermost M5-branes hit the boundaries in a second small instanton transition and so on. This evolution, in which the number of M5-branes drops successively in discrete steps, defines *cascade inflation* [13]. In [13], the analysis neglected the energy transferred to the boundaries by the instanton transitions and therefore worked, after each instanton transition, with a suitably modified power-law evolution

$$a_m(t) = a_m t^{p_{N_m}} , \quad t_{m-1} \leq t \leq t_m , \quad (5)$$

having different N dependent parameters p_N and V_N for each interval. The cascade inflation process terminates when the number of M5-branes in the m th phase, $N_m = N - 2m$, drops below a critical value N_K in the final K th phase. This critical value N_K is determined by the exit condition $p_{N_K} = 1$, at which inflation stops and which is dynamically reached from larger powers $p_{N_m} \geq p_{N_K}$, $m \leq K$. Thus we have a finite number $m = 1, \dots, K$ of cascade inflation bouts.

Throughout the whole cascade inflation process the inflaton, Δx , representing the distance between neighboring bulk M5-branes, grows continuously. Matching the scale factors at the transition times, t_m , determines the prefactors

$$a_m = a_1 t_1^{p_{N_1} - p_{N_2}} t_2^{p_{N_2} - p_{N_3}} \dots t_{m-1}^{p_{N_{m-1}} - p_{N_m}} , \quad (6)$$

where $t_{ij} = t_i/t_j$. The scale factor, but not the Hubble parameter, is continuous at the transition times t_m , when the ET to the boundaries is neglected. The onset time of inflation, t_0 , is determined by inverting the power-law inflation solution for $\varphi(t)$ in the initial phase and noting that $\Delta x(t_0)/L \ll 1$. The result is

$$t_0 \simeq \frac{2N^2}{3M_{\text{P}}^2} \sqrt{\frac{2td}{s}} . \quad (7)$$

Inverting the solution for $\varphi(t)$ gives the transition times

$$(t_m - t_0)M_P = \left(\frac{p_{N_1}(3p_{N_1} - 1)}{N_1 - 1} e^{\frac{t}{N_1}} + \sum_{k=2}^m \frac{p_{N_k}(3p_{N_k} - 1)}{N_k - 1} e^{\frac{t}{N_k} - \frac{t}{N_{k-1}}} \right) \sqrt{\frac{st^3 d}{6}}, \quad (8)$$

from which the number of e-foldings, generated during cascade inflation, derives

$$N_e = \ln \left(\frac{a(t_f)}{a(t_0)} \right) = \sum_{m=1}^K p_{N_m} \ln(t_{m,m-1}). \quad (9)$$

The analysis of [13] neglected the backreaction of the energy, which gets lost to the boundaries. The reason for this was the still open question how the small instanton transitions should be described dynamically at a fundamental level plus the naive expectation that, as long, as the number of M5-branes, having been absorbed by the boundaries, stays small compared to those remaining in the bulk and driving inflation, this might be a useful approximation. For the type I string, possessing an $SO(32)$ gauge group, the small $SO(32)$ instanton is nothing but a D5-brane in ten dimensions [57]. When compactified on a K3 manifold from ten to six dimensions, a six-dimensional instanton arises from the D5-brane wrapping the K3 which describes an effective string in six dimensions (as the string theory situation is best understood in six dimensions, we stick to this case for this brief discussion). At a certain point in moduli space the tension of this string vanishes and a singularity occurs. At this point the string's sigma model coupling is of order one, hence the sigma model is strongly coupled, whereas the string coupling constant could be arbitrarily small [57]. The type I - heterotic duality relates this type I phenomena to a singularity involving the fundamental $SO(32)$ heterotic string in six dimensions. Furthermore, invoking T-duality, one can relate the phenomenon further to the $E_8 \times E_8$ heterotic string in six dimensions [56], for which at the singularity one of the two E_8 gauge couplings diverges and the string associated with the small instanton in that gauge group becomes tensionless, while the other E_8 gauge coupling remains finite.

In heterotic M-theory, compactified on $K3 \times \mathbf{S}^1/\mathbf{Z}_2$ from eleven down to six dimensions, the two E_8 gauge groups are geometrically separated and localized on the ends of the $\mathbf{S}^1/\mathbf{Z}_2$ interval. For these we can first of all have the same instanton in either E_8 gauge theory as for the weakly coupled $E_8 \times E_8$ heterotic string with the associated tensionless string when the E_8 instanton shrinks and produces a singularity. However, a novel situation arises from the presence of M5-branes, which are generically needed to cancel anomalies. In six dimensions, these M5-branes are located as points on the compactification manifold $K3 \times \mathbf{S}^1/\mathbf{Z}_2$. An M2-brane stretches along $\mathbf{S}^1/\mathbf{Z}_2$ from the M5-brane to each boundary. Such an M2-brane

produces a string in the non-compact six dimensions, and generates a tensionless string once the M5-brane hits a boundary [56], [57]. In heterotic M-theory compactifications on $\mathbf{X} \times \mathbf{S}^1/\mathbf{Z}_2$ down to four dimensions, the small instantons are described by a torsion free sheaf, a singular bundle. The singular torsion free sheaf can then be smoothed out to a non-singular holomorphic vector bundle by moving in moduli space [54].

To date, unfortunately, no clear fundamental M-theory description of these small instanton transitions is available, which would fully describe its dynamics, including the produced tensionless strings. In what follows, switching back to a four dimensional analysis of the ensuing cosmology, we will therefore adopt a quantum field theory description which models such a transition by coupling the inflaton φ to another field χ (which in heterotic M-theory would come from the boundary). To allow for an energy transfer from the inflaton φ to the boundary field χ , we will introduce a suitable coupling between the two fields.

3 The Two Field Model

3.1 The Potential

As mentioned above, repulsive M2-instanton interactions cause the M5-branes to spread over the $\mathbf{S}^1/\mathbf{Z}_2$ interval until the two outermost M5-branes hit the interval's boundaries. The ensuing non-perturbative small instanton transition transforms the outermost M5-branes into small instantons on the boundaries [53]. This process changes the topological data on the boundaries while the number N of M5-branes, participating in the inflationary bulk dynamics, drops to $N - 2$ at each such transition. The resulting features in the inflaton's potential lead to interesting new observational phenomena. These have been derived in [13] under neglect of the full backreaction of the energy which gets transferred to the boundaries. To get a first clue how this backreaction alters the observational signatures of [13], we will now introduce a simple two field model which allows us to study the backreaction effects numerically. In our subsequent analysis we will restrict ourselves to a single collision, i.e. a single step in the inflaton potential. Furthermore, to obtain a numerically treatable model in which we can study the cosmological implications of the ET, our model will be based on just two degrees of freedom, the inflaton φ and a scalar field χ , representing the energy absorbing boundary.

The field χ is used to model in field theory a variety of boundary barotropic fluids by endowing χ with a suitable exponential potential, as we now explain. Since we do not know the equation of state of the interacting tensionless strings which are being produced in the

small instanton transitions and into which the energy of the inflaton is fed, one would like to adopt a general barotropic perfect fluid with equation of state

$$P = w\rho, \quad (10)$$

which will absorb part of the inflaton's energy. The influence of the ET on the cosmological perturbations can then be studied for various values of the parameter w . This way one could e.g. model radiation, matter or cosmic strings as possible effective components being generated on the brane in the collision. Now in a field theory framework one should rather describe the perfect fluid by a suitable field. In fact, it had been shown in [49] that a scalar field χ with an exponential potential

$$V(\chi) \sim e^{-\sqrt{\frac{2}{q}} \frac{\chi}{M_{\text{P}}}} \quad (11)$$

leads to a power-law evolution of the scale-factor, $a(t) \sim t^q$, even when $\frac{1}{3} \leq q \leq 1$. This type of evolution would also result from a perfect fluid with equation of state parameter

$$w = \frac{2}{3q} - 1. \quad (12)$$

Hence we will model the perfect fluid in a field theory description by the scalar χ together with the above exponential potential. The reader should bear in mind that the energy content of the fluids are subdominant with respect to the inflaton's energy and thus the transferred energy does not dominate the evolution of the background. Our work thus differs from others, such as [59], in that respect.

Our potential for the two scalar field model

$$V(\varphi, \chi) = V(\varphi) + W(\chi, \varphi) \quad (13)$$

consists therefore of two different components. First, there is the inflaton potential

$$V(\varphi) = v(\varphi) \exp\left(-\sqrt{\frac{2}{p(\varphi)}} \frac{(\varphi - \varphi_s)}{M_{\text{P}}}\right), \quad (14)$$

with φ_s being the value of the inflaton at the step (brane collision). This type of potential results from an M5-brane collision in cascade inflation, see eq. (2). The amplitude V_N and parameter p_N vary with N in a collision. We model this step-like variation using an inflaton dependent amplitude and parameter (the index i refers to the initial state before hitting the step, whereas the index f refers to the final state after hitting the step)

$$v(\varphi) = \frac{U_f + U_i}{2} + \frac{U_f - U_i}{2} \tanh\left(\frac{\varphi - \varphi_s}{\Delta\varphi}\right) \quad (15)$$

$$p(\varphi) = \frac{p_f + p_i}{2} + \frac{p_f - p_i}{2} \tanh\left(\frac{\varphi - \varphi_s}{\Delta\varphi}\right) \quad (16)$$

with a tanh dependence, which interpolates between -1 and 1 and smoothes the step, while the parameter $\Delta\varphi$ governs the smoothed step's width. As said earlier, we will, for simplicity, focus our attention on a single step (single brane collision) in the inflaton's potential.

Second, there is the scalar χ which has to absorb a certain amount of energy in the course of the collision, as can be seen as follows. Before the collision, there exists only the inflaton, φ , with an exponential potential with parameter p_i and amplitude U_i . During inflation the inflaton's value increases until it approaches the step at a value φ_s . Here the exponent drops to p_f and the potential's amplitude to U_f . The difference between initial and final inflaton potential energy has to be absorbed by the boundary fluid, i.e. is transferred to the field, χ . The potential for χ should be of the form given in eq. (11) for the reasons explained above. However, since energy is transferred to χ , the amplitude of its potential will change in time and thus depend on φ . Similarly, we can expect the nature of the fluid to change during the collision as e.g. a tensionless string component is created which hadn't been there before the collision. Therefore, we model the potential for χ by

$$W(\chi, \varphi) = w(\varphi) \exp\left(-\sqrt{\frac{2}{r(\varphi)}} \frac{\chi}{M_{\text{P}}}\right), \quad (17)$$

with inflaton dependent amplitude $w(\varphi)$ and parameter $r(\varphi)$. These are again expressed in terms of tanh functions

$$w(\varphi) = \frac{U_i - U_f}{2} \left(1 + \tanh\left(\frac{\varphi - \varphi_s}{\Delta\varphi}\right)\right) \quad (18)$$

$$r(\varphi) = \frac{q + p_i}{2} + \frac{q - p_i}{2} \tanh\left(\frac{\varphi - \varphi_s}{\Delta\varphi}\right) \quad (19)$$

to describe a smoothed out step. In this way we arrive at a coupling between φ and χ .

Before encountering the step, the scalar χ describes a fluid with equation of state parameter $w_i = \frac{2}{3p_i} - 1$. The potential of χ is almost zero because its amplitude is almost vanishing. This changes quickly during the collision, at which the amplitude raises to $U_i - U_f$ (the ET coming from the inflaton) and the equation of state parameter soon adjusts itself at $w = \frac{2}{3q} - 1$. In what follows, we will mostly focus on the case where the inflaton's energy is transferred to an effective radiation component ($q = 1/2$) but will also consider matter ($q = 2/3$) or a network of cosmic strings component ($q = 1$). We concentrate on the radiation case first and choose for definiteness the following parameter values

$$p_i = 40.138, \quad p_f = 36.598, \quad \frac{(U_i - U_f)}{U_i} = 0.068, \quad (20)$$

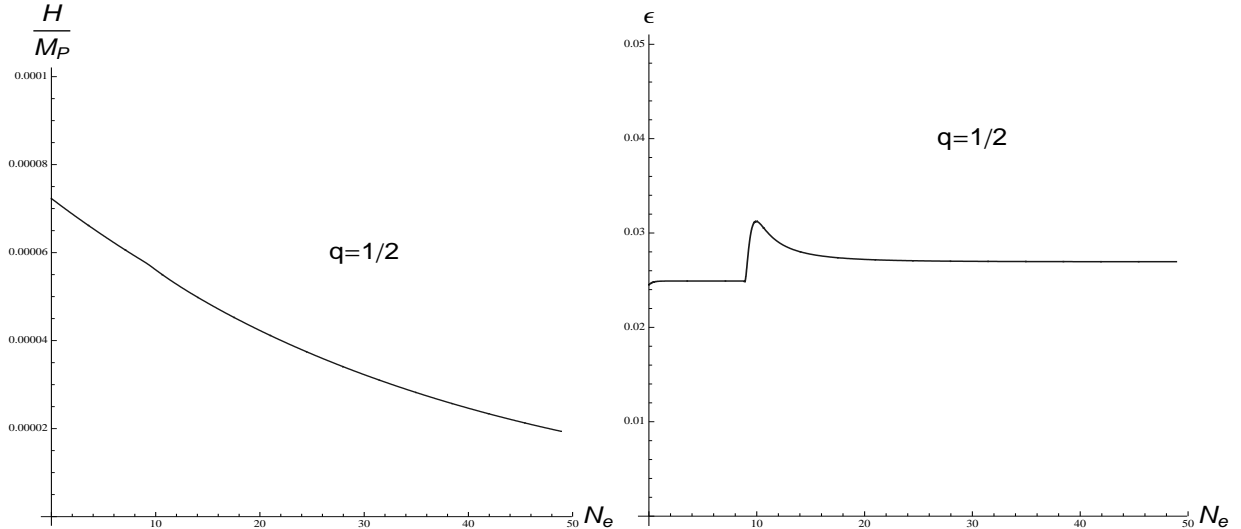


Figure 1: The graphs show the evolution of the Hubble parameter and the first slow-roll parameter as a function of the number of e-foldings. Around $N_e \simeq 10$ the inflaton's potential energy ($U_i - U_f$) is transferred to the χ field.

$$\varphi_s = 1.477 M_P, \quad \Delta\varphi = 10^{-3} M_P. \quad (21)$$

The initial value of χ is chosen to be zero, $\chi_i = 0$, such that the inflaton's potential energy $U_i - U_f$ is transferred to the χ field.

3.2 Cosmological Evolution

Fig. 1 shows the evolution of the Hubble parameter and the first slow-roll parameter of the model as a function of the number of e-foldings. Around $N_e \simeq 10$ the step is encountered (brane collision takes place) and the fraction $(U_i - U_f)/U_i$ of the inflaton's potential energy is transferred to the χ field. Since the χ direction in the total potential $V(\varphi, \chi)$ is much steeper than the inflaton direction, its energy content redshifts within a few e-foldings and the background evolves solely under the influence of the final inflaton potential

$$V(\varphi) \rightarrow U_f \exp\left(-\sqrt{\frac{2}{p_f}} \frac{(\varphi - \varphi_s)}{M_P}\right) \quad (22)$$

after that. As the slope of the potential increases after the energy of χ redshifts, the slow-roll parameter, ϵ , settles to a slightly larger value, see the right graph in fig. 1.

The trajectory of φ and χ in field space and the evolution of their combination θ , which had been defined in eq. (44), is graphed in fig. 2. There is a sharp turn in the classical trajectory of the fields, when the inflaton, φ , transfers part of its energy to χ . As we will

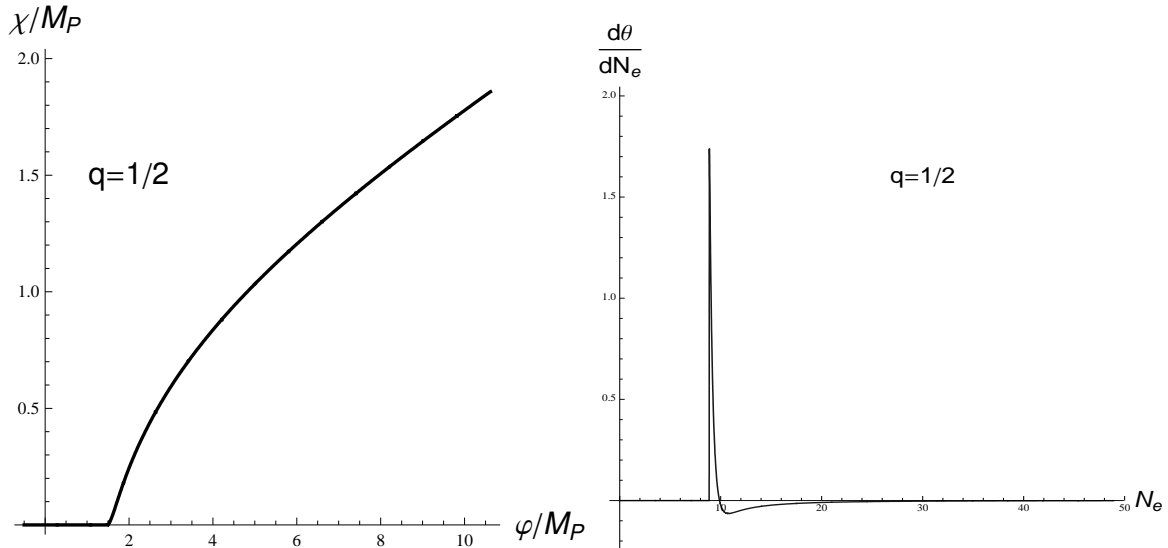


Figure 2: The left graph shows the evolution of the fields φ and χ . They move upwards from left to right along the black trajectory, whose very first part coincides with the φ axis. The right graph displays $d\theta/dN_e$ as a function of the number of e-foldings N_e . A sharp turn in field space at the collision is clearly visible.

see, with this bent in the trajectory, the curvature perturbations are strongly fed by entropy perturbations. We will now calculate the curvature and isocurvature spectra for our energy exchanging two field model.

4 Adiabatic and Isocurvature Perturbations

For the two-field model described above, we integrate the equations of motion for the curvature and the isocurvature perturbations, eqs. (55) and (56), whose derivation is outlined in Appendix.

4.1 Evolution of Curvature and Entropy Perturbations.

Fig. 3 shows the result for the evolution of curvature and entropy fluctuations for two modes: one that exits the horizon before the ET at $\log(k/a_0H_0) = 7.5$, and a second mode which exits it after the ET at $\log(k/a_0H_0) = 10.5$. The subscript 0 denotes the values of the scale factor and Hubble parameter at the beginning of inflation. Since we have to deal with two independent physical degrees of freedom, we perform the integration twice to account for the two independent quantum fluctuations. In the first run, we assume that Q_σ is initially in the Bunch-Davies vacuum and that δs initially vanishes. In this manner, we obtain the

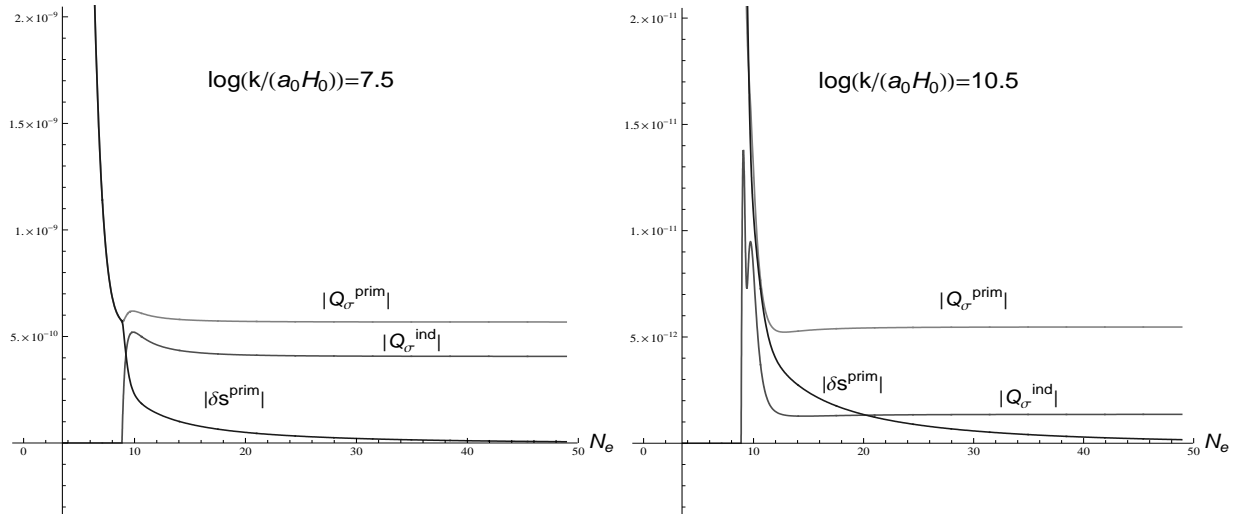


Figure 3: The left and right graphs show the evolution of $|Q_\sigma^{\text{prim}}|$, $|Q_\sigma^{\text{ind}}|$ and $|\delta s^{\text{prim}}|$ as functions of N_e for two comoving wave-numbers that exit the horizon before respectively after the ET.

primordial curvature perturbations Q_σ^{prim} and the induced isocurvature perturbations δs^{ind} . In the second run we interchange the initial conditions for Q_σ and δs to obtain Q_σ^{ind} and δs^{prim} . The total amplitude of the curvature perturbations is given by:

$$|Q_\sigma^{\text{tot}}|^2 = |Q_\sigma^{\text{ind}}|^2 + |Q_\sigma^{\text{prim}}|^2 \quad (23)$$

and the amplitude of the total isocurvature perturbations is given by an analogical expression. In the single-field case, we perform just one integration.

Deep inside the Hubble radius, the two perturbations evolve independently in the same way, up to a slow overall rotation which practically does not change the amplitudes or the correlations. After the Hubble radius crossing $|Q_\sigma^{\text{prim}}|$ approaches the value it would have obtained in absence of any isocurvature perturbations. The induced perturbations, Q_σ^{ind} and δs^{ind} are practically negligible inside the Hubble radius. The former can be generated on the super-Hubble scales, where its EOM in the slow-roll approximation reads [61, 44]:

$$\frac{1}{H} \dot{\mathcal{R}} = \frac{k^2}{\dot{H} a^2} \Phi - \frac{2}{H} \dot{\theta} \mathcal{S}, \quad (24)$$

given that the background trajectory in the field space is sufficiently curved. Also $|Q_\sigma^{\text{ind}}|$ for such modes is much smaller than Q_σ^{prim} and consequently we do not see considerable enhancement at such scales.

The behavior of the field valued function $d\theta/dN$ is displayed in the right graph of fig. 2. Before the ET, this function is zero and thus no induced curvature perturbations, $|Q_\sigma^{\text{ind}}|$, are

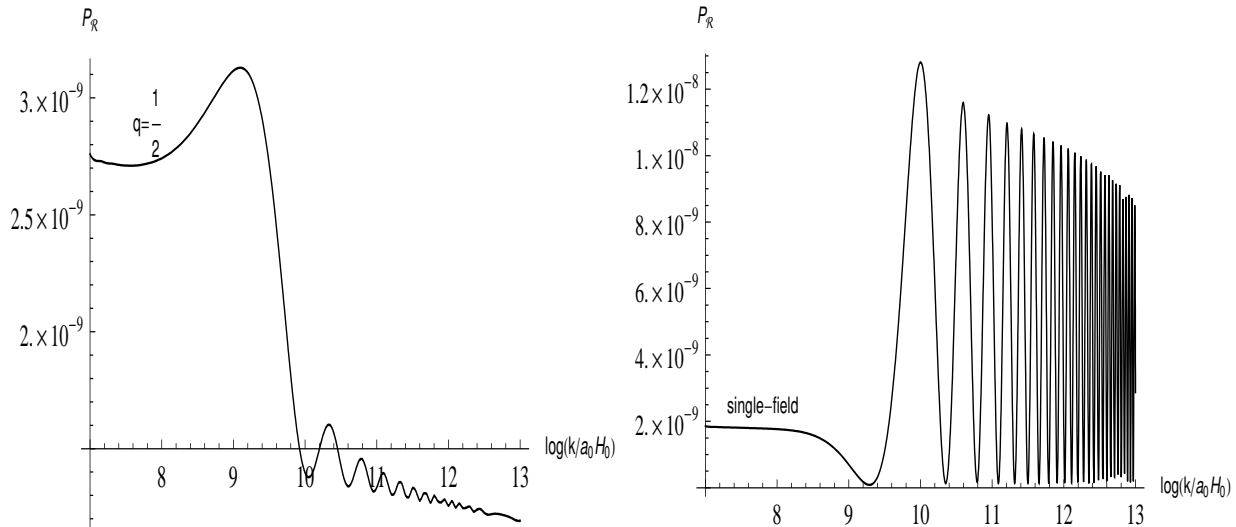


Figure 4: The left graph shows the adiabatic spectrum vs. $\log(k/a_0 H_0)$ for the modes that exit the horizon around the decay time. It is assumed that the energy of the decay products redshifts as radiation, $U_f/U_i = 0.932$ and $\Delta\phi = 10^{-3} M_{\text{P}}$. The right graph shows the adiabatic power spectrum for the single field case with an inflaton potential having a step of equal height. The oscillations in the single field case last much longer than in the two field case with ET.

generated. As the ET from φ to χ happens, the sharp turn in the classical trajectory creates a spike in $d\theta/dN$. This will lead to a considerable increment in the curvature perturbations on super-Hubble scales, due to interaction with isocurvature perturbations. As the energy of the χ -field redshifts, $d\theta/dN$ becomes zero again and the amplitude $|Q_\sigma^{\text{ind}}|$ becomes frozen. This results in an overall enhancement of the amplitude of the curvature modes that exit the horizon before the ET. For modes that exit the horizon after the ET, the function $|Q_\sigma^{\text{ind}}|$ undergoes some modulated oscillations before becoming constant at super-horizon scales. As we will see, these oscillations will imprint themselves as modulated oscillations on the curvature spectrum.

4.2 Curvature and Entropy Spectra

The left plot of fig. 4 demonstrates the dependence of the adiabatic spectrum on $\log(k/a_0 H_0)$. For comparison, we have also shown the power spectrum for a single inflaton model with exponential potential possessing a step of same height. This model is obtained by setting the potential for the χ field, $W(\chi, \varphi)$, and therefore also the coupling to φ , to zero. The height of the potential step in the single field case is entirely transferred into kinetic energy of the inflaton [60]. One point that easily gets noticed by comparing these two graphs is

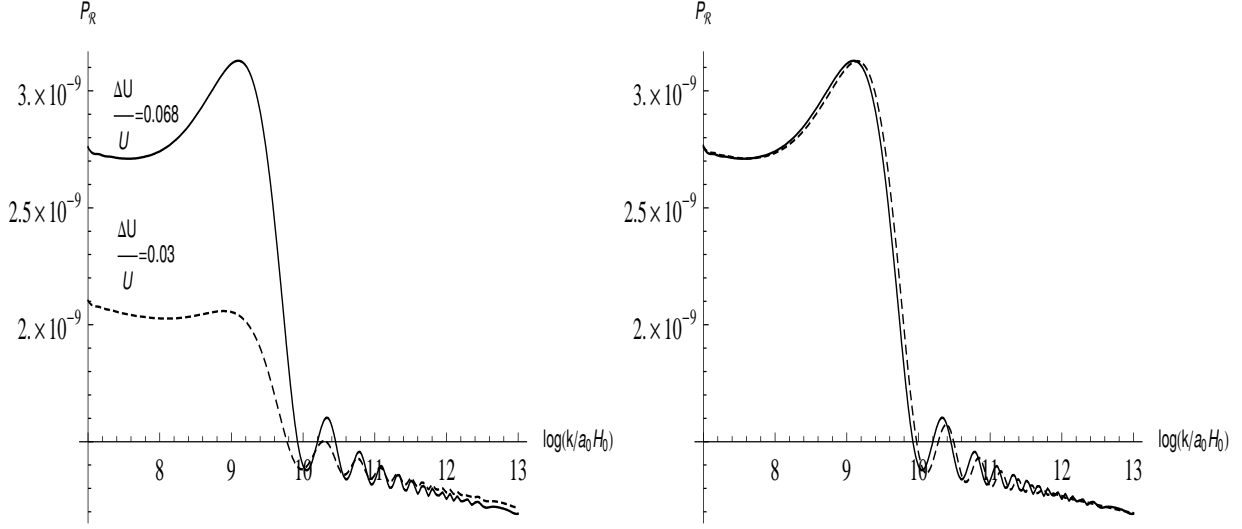


Figure 5: The left graph shows the curvature spectra vs. $\log(k/a_0 H_0)$ for $\Delta U/U_i = 0.068$ and $\Delta U/U_i = 0.03$. The right graph shows the adiabatic power spectra vs. $\log(k/a_0 H_0)$ for $\Delta\varphi = 10^{-2}M_{\text{P}}$ (black solid line) and $\Delta\varphi = 10^{-3}M_{\text{P}}$ (dashed grey line)

that the modulated oscillations in the power spectrum for the two field case decay much faster than in the single field case. For $U_f/U_i = 0.932$, the modulated oscillations last for four decades in k for the two field case, whereas in the single field case they continue for more than eight decades. Also the amplitude of those modes that exit the horizon before the decay is increased by 41%. As mentioned above, this is due to the strong interaction of the adiabatic and isocurvature perturbations, when part of the inflaton's energy is transferred to χ .

In the slow roll approximation, the EOM of the isocurvature perturbations on the super-Hubble scales can be approximated by:

$$\frac{d\delta s}{dN_e} \simeq -\eta_{ss}\delta s. \quad (25)$$

Since the potential is typically much more curved in the direction orthogonal to the trajectory in the field space than in the direction along the trajectory. Hence, the isocurvature perturbations decay exponentially from their corresponding value at the horizon crossing. The shape of the isocurvature spectrum is given in fig. 6. Their corresponding value is sub-dominant with respect to the curvature perturbations by a factor which varies between 10^{-3} to 10^{-4} at different scales. One can see a slight amplification followed by modulated oscillation at the scales that leave the horizon around the ET.

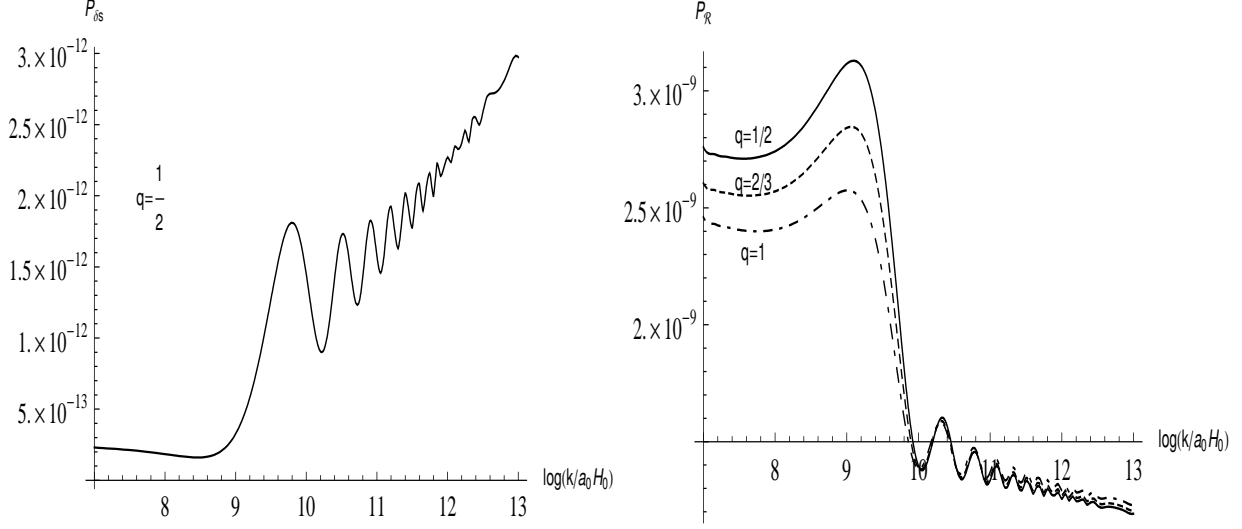


Figure 6: The left graph shows the entropy spectrum vs. $\log(k/a_0 H_0)$ for $\Delta U/U_i = 0.932$ and $\Delta\varphi = 10^{-3} M_P$. The right graph shows the dependence of the adiabatic spectrum on q .

We now consider the effect of changing

$$\Delta U/U \equiv (U_i - U_f)/U_i, \quad (26)$$

keeping all other parameters constant. The left graph of fig. 5 shows the adiabatic spectra for $\Delta U/U = 0.068$ and $\Delta U/U = 0.03$. Reducing the energy which gets transferred to the χ field by a factor of ~ 2.25 , decreases the amount of increment in the adiabatic perturbations at wave numbers smaller than $k_{ET} \equiv aH|_{ET}$ by a factor of ~ 4.2 . The amplitude of the modulated fluctuations at $k > k_{ET}$ decreases too, even though the frequency of the oscillations remains more or less the same.

We also considered the effect of changing the parameter $\Delta\varphi$ which physically corresponds to the decay width of the inflaton. The result is displayed in the right graph of fig. 5. The smaller this parameter is, the faster the energy from inflaton, φ , transfers to χ . By decreasing this parameter, the adiabatic power spectrum is shifted slightly toward larger scales. This is intuitively understandable, as in this case the inflaton energy, ΔU , is exchanged faster and thus the resulting oscillations start at larger scales.

So far we have assumed that the decay product χ has a potential which makes it redshift like radiation, $q = 1/2$. We now relax this constraint and consider how the perturbations will evolve if we choose q appropriate for matter, $q = 2/3$, or a web of cosmic strings, $q = 1$. Fig.(6) shows how the curvature spectrum changes once χ decays like radiation. For a fixed amount of energy transferred to χ field, increasing q , reduces the amount of amplification

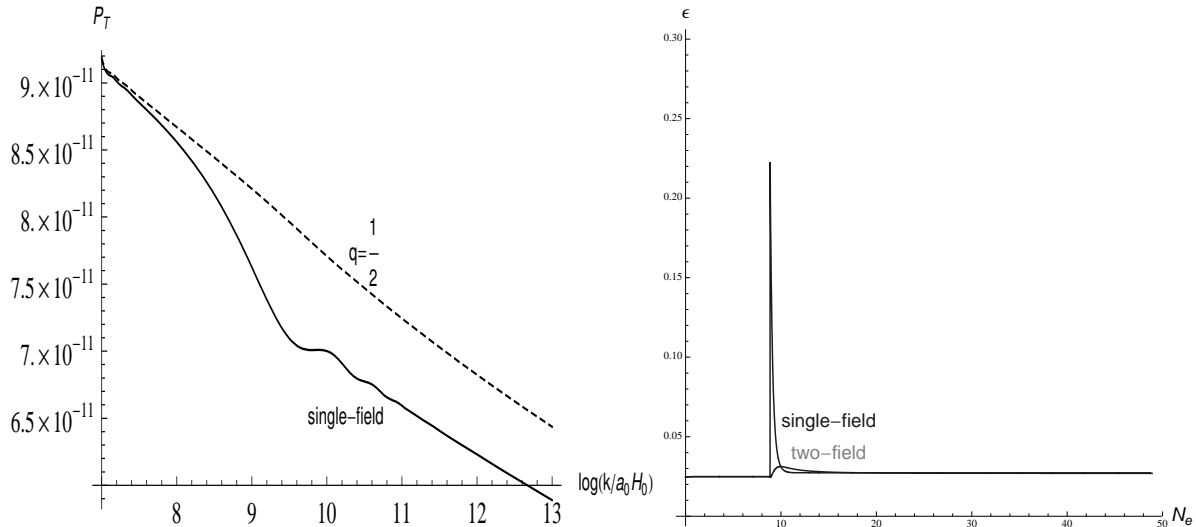


Figure 7: The left graph shows the tensor spectra vs. $\log(k/a_0 H_0)$ for $\Delta U/U_i = 0.932$. Solid and dashed lines respectively represent the single field and two field cases. The right plot shows the dependence of the slow-roll parameter ϵ on N_e .

of curvature spectrum at wave-numbers $k < k_{\text{ET}}$. Thus the least amount of amplification at such scales occurs for $q = 1$. The amplitude and frequency of the oscillations are more or less independent from parameter q .

4.3 Tensor Spectrum

Finally, we are investigating the tensor spectra of the energy exchanging two field inflation model. The left plot of fig. 7 shows the profile of gravity waves for the modes that exit the horizon during the ET. For comparison we have also plotted the tensor spectrum for the single field case, in which the energy of the step in the φ potential is snatched by the kinetic energy of φ itself. In the single field case the spectrum displays some oscillations for the modes that exit the horizon around the ET. This could be understood by comparing the variations of ϵ for the two cases. Tensor perturbations satisfy the following equation [62]

$$p_k'' + \left(k^2 - \frac{a''}{a} \right) p_k = 0. \quad (27)$$

The quotient a''/a can be written in terms of the slow-roll parameter ϵ as

$$\frac{a''}{a} = 2a^2 H^2 (2 - \epsilon). \quad (28)$$

To understand its implication for the tensor spectrum, we exhibit in the right plot of fig. 7 the evolution of ϵ with N_e for the two field and single field cases. In both cases, during the

non-slow-roll phases, there are sharp spikes in ϵ . However, for the single field case, the spike in ϵ is much greater than in the two field case. This large variation in ϵ in the single field case leads to modulated wiggles on the amplitude of its tensor spectrum and explains the difference between the single and two field cases seen in the left part of fig. 7.

This result for the single field case should be contrasted with the results of [60], where no observable signature in the tensor power spectrum had been observed. However, one should note that the energy difference in the step was chosen much smaller in [60] and thus ϵ would not exhibit such a sharp spike.

Furthermore, it can be seen from the left plot in fig. 7 that the amplitude of the tensor spectrum decays much faster in the single field than in the two field case. This is because the liberated energy from the potential's step transforms in the single field case to the kinetic energy of the inflaton φ , which redshifts like a^{-6} . On the contrary, in the two field case the released energy is absorbed by the χ field which redshifts much slower. This will cause the the Hubble parameter in the single field case to diminish much faster. As the amplitude of the tensor perturbation is roughly given by $H/2\pi$, this explains the smallness of the tensor spectra in the single field case compared to the larger tensor spectra of the two field case which we see in the left plot of fig. 7.

Acknowledgments

A.A. is partially supported by the Natural Sciences and Engineering Research Council of Canada. A.K. is supported by the German Research Foundation (DFG) and the Transregional Collaborative Research Centre TR33 “The Dark Universe”. K.T. is partially supported by the grant MNiSW N202 176 31/3844 and by TOK Project MTKD-CT-2005-029466. K.T. also acknowledges support from the Foundation for Polish Science through its programme HOMING.

Appendix: Curvature and Isocurvature Perturbations in Two-field Inflation

The calculation of cosmological perturbations in the multi-field inflation is an extensively studied topic. Nonetheless, we would like to review the basic notation, results and, in particular, the equations of motion for the perturbations that we solve numerically. In this section, we shall follow closely the presentation of [41].

A two-scalar-field system coupled to gravity is described by an action of the form

$$S = \int d^4x \sqrt{-g} \left(\frac{M_{\text{P}}^2}{2} R - \frac{1}{2} \partial_\mu \varphi \partial^\mu \varphi - \frac{1}{2} \partial_\mu \chi \partial^\mu \chi - V(\varphi, \chi) \right), \quad (29)$$

where M_{P} is the reduced Planck mass, $M_{\text{P}} \equiv (8\pi G)^{-1/2}$. The homogeneous and isotropic FRW background with metric

$$ds^2 = -dt^2 + a(t)^2 d\mathbf{x}^2, \quad (30)$$

is governed by the equations of motion (EOM) for the two scalar fields:

$$\ddot{\varphi} + 3H\dot{\varphi} + V_{,\varphi} = 0 \quad (31)$$

$$\ddot{\chi} + 3H\dot{\chi} + V_{,\chi} = 0. \quad (32)$$

Subscripts φ and χ denote partial derivatives with respect to the corresponding field and a dot denotes a derivative with respect to the cosmic time, t . The gravitational background evolves according to Friedmann-Lemâitre equations:

$$H^2 = \frac{1}{3M_{\text{P}}^2} \left(\frac{1}{2} \dot{\varphi}^2 + \frac{1}{2} \dot{\chi}^2 + V(\varphi, \chi) \right) \quad (33)$$

$$\dot{H} = -\frac{1}{2M_{\text{P}}^2} (\dot{\varphi}^2 + \dot{\chi}^2), \quad (34)$$

where H is the Hubble parameter, defined as $H \equiv \frac{\dot{a}}{a}$.

To study the linear perturbations for this theory, we start with the longitudinal gauge for the metric [43]. In the absence of any anisotropic stress-energy tensor the scalar perturbation of the gravitational background reads:

$$ds^2 = -(1 + 2\Phi(t, \mathbf{x})) dt^2 + a(t)^2 (1 - 2\Phi(t, \mathbf{x})) d\mathbf{x}^2. \quad (35)$$

The scalar fields are also perturbed around their homogeneous parts,

$$\varphi(t, \mathbf{x}) = \varphi(t) + \delta\varphi(t, \mathbf{x}) \quad \text{and} \quad \chi(t, \mathbf{x}) = \chi(t) + \delta\chi(t, \mathbf{x}), \quad (36)$$

These perturbations introduce an \mathbf{x} dependence which was not present in the homogeneous and isotropic gravitational and scalar field backgrounds. To determine the perturbations, one therefore has to insert the perturbed metric and scalar fields into the full Einstein field equations and/or Bianchi identities, and the full scalar field EOMs.

Since the perturbations of the metric and the scalar fields are not independent, it is useful to introduce gauge-invariant Mukhanov-Sasaki variables

$$Q_\varphi \equiv \delta\varphi + \frac{\dot{\varphi}}{H} \Phi \quad \text{and} \quad Q_\chi \equiv \delta\chi + \frac{\dot{\chi}}{H} \Phi. \quad (37)$$

They represent the scalar field fluctuations in the flat gauge. It follows from the EOMs that their Fourier-components obey the coupled differential equations²

$$\ddot{Q}_\varphi + 3H\dot{Q}_\varphi + \left(\frac{k^2}{a^2} + C_{\varphi\varphi}\right) Q_\varphi + C_{\varphi\chi} Q_\chi = 0 \quad (38)$$

$$\ddot{Q}_\chi + 3H\dot{Q}_\chi + \left(\frac{k^2}{a^2} + C_{\chi\chi}\right) Q_\chi + C_{\chi\varphi} Q_\varphi = 0, \quad (39)$$

with the following background-dependent coefficients

$$C_{\varphi\varphi} = \frac{3\dot{\varphi}^2}{M_{\text{P}}^2} - \frac{\dot{\varphi}^2\dot{\chi}^2}{2M_{\text{P}}^4H^2} - \frac{\dot{\varphi}^4}{2M_{\text{P}}^4H^2} + \frac{2\dot{\varphi}V_\varphi}{M_{\text{P}}^2H} \quad (40)$$

$$C_{\varphi\chi} = \frac{3\dot{\varphi}\dot{\chi}}{M_{\text{P}}^2} - \frac{\dot{\varphi}\dot{\chi}^3}{2M_{\text{P}}^4H^2} - \frac{\dot{\varphi}^3\dot{\chi}}{2M_{\text{P}}^4H^2} + \frac{\dot{\varphi}V_\chi}{M_{\text{P}}^2H} + \frac{\dot{\chi}V_\varphi}{M_{\text{P}}^2H} + V_{\varphi\chi} \quad (41)$$

$$C_{\chi\chi} = \frac{3\dot{\chi}^2}{M_{\text{P}}^2} - \frac{\dot{\chi}^4}{2M_{\text{P}}^4H^2} - \frac{\dot{\varphi}^2\dot{\chi}^2}{2M_{\text{P}}^4H^2} + \frac{\dot{\chi}V_\chi}{M_{\text{P}}^2H} + V_{\chi\chi} \quad (42)$$

$$C_{\chi\varphi} = \frac{3\dot{\varphi}\dot{\chi}}{M_{\text{P}}^2} - \frac{\dot{\varphi}\dot{\chi}^3}{2M_{\text{P}}^4H^2} - \frac{\dot{\varphi}^3\dot{\chi}}{2M_{\text{P}}^4H^2} + \frac{\dot{\varphi}V_\chi}{M_{\text{P}}^2H} + \frac{\dot{\chi}V_\varphi}{M_{\text{P}}^2H} + V_{\varphi\chi}. \quad (43)$$

Following [44], we decompose the perturbations along and perpendicular to the trajectory in the (homogeneous) field space. The projection parallel to the trajectory is called the instantaneous curvature, or adiabatic, perturbation whereas the one orthogonal to the trajectory is termed the instantaneous isocurvature, or entropy, perturbation. The velocity in the field space is $\dot{\sigma} \equiv \sqrt{\dot{\varphi}^2 + \dot{\chi}^2}$ and we can define the polar angle in the field space as

$$\cos \theta \equiv \dot{\varphi} / \dot{\sigma} \quad (44)$$

It is now useful to define the following Mukhanov-Sasaki variable:

$$Q_\sigma = \cos \theta Q_\varphi + \sin \theta Q_\chi. \quad (45)$$

In the flat gauge, Q_σ represent the field perturbations along the velocity in the field space. Q_σ is also related to the commonly used curvature perturbation, \mathcal{R} , of the comoving hypersurface via

$$\mathcal{R} = \frac{H}{\dot{\sigma}} Q_\sigma. \quad (46)$$

Similarly the isocurvature perturbation is:

$$\delta s = -\sin \theta Q_\varphi + \cos \theta Q_\chi. \quad (47)$$

²Even though, we will work with Fourier components hereafter, we will not show explicitly the subscript \mathbf{k} which would denote the fluctuation with comoving wave-number \mathbf{k} .

It describes field perturbation perpendicular to the field velocity in the field space and, by analogy with \mathcal{R} , we can define a rescaled entropy perturbation, \mathcal{S} , through

$$\mathcal{S} = \frac{H}{\dot{\sigma}} \delta s . \quad (48)$$

The transformations described above basically amount to introducing a new orthonormal basis in the field space, defined by vectors

$$E_\sigma = (E_\sigma^\varphi, E_\sigma^\chi) = (\cos \theta, \sin \theta) , \quad (49)$$

$$E_s = (E_s^\varphi, E_s^\chi) = (-\sin \theta, \cos \theta) , \quad (50)$$

which turn out to be useful to express various derivatives of the potential with respect to the curvature and isocurvature perturbations. Employing an implicit summation over the indices $I, J \in \{\varphi, \chi\}$, one thus finds

$$V_\sigma = E_\sigma^I V_I , \quad V_s = E_s^I V_I , \quad (51)$$

and

$$V_{\sigma\sigma} = E_\sigma^I E_\sigma^J V_{IJ} , \quad V_{\sigma s} = E_\sigma^I E_s^J V_{IJ} , \quad V_{ss} = E_s^I E_s^J V_{IJ} . \quad (52)$$

for the first and second derivatives.

By combining the Klein-Gordon equations for the background scalar fields, eqs. (31) and (32), one obtains the background EOMs along the curvature and isocurvature directions

$$\frac{d\dot{\sigma}}{dt} + 3H\dot{\sigma} + V_\sigma = 0, \quad (53)$$

$$\dot{\theta} = -\frac{V_s}{\dot{\sigma}} . \quad (54)$$

With help of these one can show that the EOMs for curvature and isocurvature perturbations become

$$\ddot{Q}_\sigma + 3H\dot{Q}_\sigma + \left(\frac{k^2}{a^2} + C_{\sigma\sigma} \right) Q_\sigma + \frac{2V_s}{\dot{\sigma}} \dot{\delta}s + C_{\sigma s} \delta s = 0, \quad (55)$$

$$\ddot{\delta}s + 3H\dot{\delta}s + \left(\frac{k^2}{a^2} + C_{ss} \right) \delta s - \frac{2V_s}{\dot{\sigma}} \dot{Q}_\sigma + C_{s\sigma} Q_\sigma = 0, \quad (56)$$

with coefficients given by

$$C_{\sigma\sigma} = V_{\sigma\sigma} - \left(\frac{V_s}{\dot{\sigma}}\right)^2 + \frac{2\dot{\sigma}V_\sigma}{M_{\text{P}}^2H} + \frac{3\dot{\sigma}^2}{M_{\text{P}}^2} - \frac{\dot{\sigma}^4}{M_{\text{P}}^4H^2} \quad (57)$$

$$C_{\sigma s} = 6H\frac{V_s}{\dot{\sigma}} + \frac{2V_\sigma V_s}{\dot{\sigma}^2} + 2V_{\sigma s} + \frac{\dot{\sigma}V_s}{M_{\text{P}}^2H} \quad (58)$$

$$C_{ss} = V_{ss} - \left(\frac{V_s}{\dot{\sigma}}\right)^2 \quad (59)$$

$$C_{s\sigma} = -6H\frac{V_s}{\dot{\sigma}} - \frac{2V_\sigma V_s}{\dot{\sigma}^2} + \frac{\dot{\sigma}V_s}{M_{\text{P}}^2H} . \quad (60)$$

A solution to these two coupled differential equations determines the metric perturbation Φ , which, in longitudinal gauge, is related to the comoving energy density

$$\epsilon_m = \dot{\sigma}\dot{Q}_\sigma + \left(3H + \frac{\dot{H}}{H}\right)\dot{\sigma}Q_\sigma + V_\sigma Q_\sigma + 2V_s\delta s \quad (61)$$

via the Poisson-like relation

$$\frac{k^2}{a^2}\Phi = -\frac{1}{2M_{\text{P}}}\epsilon_m . \quad (62)$$

The power spectra of curvature (adiabatic) and isocurvature (entropy) perturbations are defined, respectively, as

$$\mathcal{P}_\sigma(k) = \frac{k^3}{2\pi^2} \langle Q_{\sigma\mathbf{k}}^* Q_{\sigma\mathbf{k}'} \rangle \delta^3(\mathbf{k} - \mathbf{k}') , \quad \mathcal{P}_{\delta s}(k) = \frac{k^3}{2\pi^2} \langle \delta s_{\mathbf{k}}^* \delta s_{\mathbf{k}'} \rangle \delta^3(\mathbf{k} - \mathbf{k}') . \quad (63)$$

The curvature and isocurvature perturbations are then evolved by assuming initially, at conformal time τ_i , a Bunch-Davies vacuum. Therefore, when the wavelength of the two types of perturbations is initially much smaller than the Hubble radius, $k \gg aH$, we impose the initial conditions

$$Q_\sigma(\tau_i) = \frac{e^{-ik\tau_i}}{a(\tau_i)\sqrt{2k}} , \quad \text{and} \quad \delta s(\tau_i) = \frac{e^{-ik\tau_i}}{a(\tau_i)\sqrt{2k}} . \quad (64)$$

Inside the horizon these two modes are independent, because their corresponding EOMs, eqs. (55) and (56), are independent in the limit $k \gg aH$. However, as we will see in detail later, this does not hold when the modes leave the horizon [45, 46].

Finally, let us introduce the two field slow-roll parameters

$$\epsilon_{\varphi\varphi} = \frac{\dot{\phi}^2}{2M_{\text{P}}H^2} , \quad \epsilon_{\varphi\chi} = \frac{\dot{\phi}\dot{\chi}}{2M_{\text{P}}H^2} , \quad \epsilon_{\chi\chi} = \frac{\dot{\chi}^2}{2M_{\text{P}}H^2} \quad (65)$$

$$\eta_{IJ} = \frac{V_{IJ}}{3H^2} \quad (66)$$

and

$$\epsilon = \epsilon_{\varphi\varphi} + \epsilon_{\chi\chi} = -\frac{\dot{H}}{H^2} . \quad (67)$$

References

- [1] G. R. Dvali and S. H. H. Tye, Phys. Lett. B **450**, 72 (1999) [arXiv:hep-ph/9812483].
- [2] S. Kachru, R. Kallosh, A. Linde, J. M. Maldacena, L. P. McAllister and S. P. Trivedi, JCAP **0310**, 013 (2003) [arXiv:hep-th/0308055].
- [3] C. P. Burgess, J. M. Cline, K. Dasgupta and H. Firouzjahi, JHEP **0703**, 027 (2007) [arXiv:hep-th/0610320].
- [4] A. Krause and E. Pajer, JCAP **0807**, 023 (2008) [arXiv:0705.4682 [hep-th]].
- [5] D. Baumann, A. Dymarsky, I. R. Klebanov and L. McAllister, JCAP **0801**, 024 (2008) [arXiv:0706.0360 [hep-th]].
- [6] M. Haack, R. Kallosh, A. Krause, A. Linde, D. Lust and M. Zagermann, Nucl. Phys. B **806**, 103 (2008) [arXiv:0804.3961 [hep-th]].
- [7] H. Y. Chen, P. Ouyang and G. Shiu, arXiv:0807.2428 [hep-th].
- [8] D. A. Easson, R. Gregory, D. F. Mota, G. Tasinato and I. Zavala, JCAP **0802**, 010 (2008) [arXiv:0709.2666 [hep-th]].
- [9] A. Misra and P. Shukla, Nucl. Phys. B **799**, 165 (2008) [arXiv:0707.0105 [hep-th]].
- [10] L. Hoi and J. M. Cline, arXiv:0810.1303 [hep-th].
- [11] K. Becker, M. Becker and A. Krause, Nucl. Phys. B **715**, 349 (2005) [arXiv:hep-th/0501130].
- [12] J. M. Cline and H. Stoica, Phys. Rev. D **72**, 126004 (2005) [arXiv:hep-th/0508029].
- [13] A. Ashoorioon and A. Krause, arXiv:hep-th/0607001.
- [14] S. Thomas and J. Ward, Phys. Rev. D **76**, 023509 (2007) [arXiv:hep-th/0702229].
- [15] A. Krause, JCAP **0807**, 001 (2008) [arXiv:0708.4414 [hep-th]].
- [16] J. Ward, JHEP **0712**, 045 (2007) [arXiv:0711.0760 [hep-th]].
- [17] S. Dimopoulos, S. Kachru, J. McGreevy and J. G. Wacker, JCAP **0808**, 003 (2008) [arXiv:hep-th/0507205].

- [18] R. Easther and L. McAllister, JCAP **0605**, 018 (2006) [arXiv:hep-th/0512102].
- [19] S. A. Kim and A. R. Liddle, Phys. Rev. D **74**, 023513 (2006) [arXiv:astro-ph/0605604].
- [20] Y. S. Piao, Phys. Rev. D **74**, 047302 (2006) [arXiv:gr-qc/0606034].
- [21] H. Singh, Mod. Phys. Lett. A **22**, 2737 (2007) [arXiv:hep-th/0608032].
- [22] S. A. Kim and A. R. Liddle, Phys. Rev. D **74**, 063522 (2006) [arXiv:astro-ph/0608186].
- [23] T. Battefeld and R. Easther, JCAP **0703**, 020 (2007) [arXiv:astro-ph/0610296].
- [24] J. O. Gong, Phys. Rev. D **75**, 043502 (2007) [arXiv:hep-th/0611293].
- [25] M. E. Olsson, JCAP **0704**, 019 (2007) [arXiv:hep-th/0702109].
- [26] D. Battefeld and T. Battefeld, JCAP **0705**, 012 (2007) [arXiv:hep-th/0703012].
- [27] S. A. Kim and A. R. Liddle, Phys. Rev. D **76**, 063515 (2007) [arXiv:0707.1982 [astro-ph]].
- [28] R. Kallosh, N. Sivanandam and M. Soroush, Phys. Rev. D **77**, 043501 (2008) [arXiv:0710.3429 [hep-th]].
- [29] G. Calcagni and A. R. Liddle, Phys. Rev. D **77**, 023522 (2008) [arXiv:0711.3360 [astro-ph]].
- [30] D. Langlois and S. Renaux-Petel, JCAP **0804**, 017 (2008) [arXiv:0801.1085 [hep-th]].
- [31] I. Ahmad, Y. S. Piao and C. F. Qiao, JCAP **0802**, 002 (2008) [arXiv:0801.3129 [astro-ph]].
- [32] D. Battefeld and S. Kawai, Phys. Rev. D **77**, 123507 (2008) [arXiv:0803.0321 [astro-ph]].
- [33] D. Langlois, S. Renaux-Petel, D. A. Steer and T. Tanaka, arXiv:0806.0336 [hep-th].
- [34] S. Watson, M. J. Perry, G. L. Kane and F. C. Adams, JCAP **0711**, 017 (2007) [arXiv:hep-th/0610054].
- [35] D. Battefeld, T. Battefeld and A. C. Davis, arXiv:0806.1953 [hep-th].
- [36] H. Y. Chen, J. O. Gong and G. Shiu, JHEP **0809**, 011 (2008) [arXiv:0807.1927 [hep-th]].

- [37] D. Langlois, arXiv:0809.2540 [astro-ph].
- [38] I. Ahmad, Y. S. Piao and C. F. Qiao, arXiv:0809.3333 [hep-th].
- [39] Y. F. Cai and W. Xue, arXiv:0809.4134 [hep-th].
- [40] A. R. Liddle, A. Mazumdar and F. E. Schunck, Phys. Rev. D **58**, 061301 (1998) [arXiv:astro-ph/9804177].
- [41] Z. Lalak, D. Langlois, S. Pokorski and K. Turzynski, JCAP **0707**, 014 (2007) [arXiv:0704.0212 [hep-th]].
- [42] F. Di Marco, F. Finelli and R. Brandenberger, Phys. Rev. D **67**, 063512 (2003) [arXiv:astro-ph/0211276].
- [43] V. F. Mukhanov, H. A. Feldman and R. H. Brandenberger, Phys. Rept. **215**, 203 (1992).
- [44] C. Gordon, D. Wands, B. A. Bassett and R. Maartens, Phys. Rev. D **63**, 023506 (2001) [arXiv:astro-ph/0009131].
- [45] S. Tsujikawa, D. Parkinson and B. A. Bassett, Phys. Rev. D **67**, 083516 (2003) [arXiv:astro-ph/0210322].
- [46] C. T. Byrnes and D. Wands, Phys. Rev. D **74**, 043529 (2006) [arXiv:astro-ph/0605679].
- [47] P. Horava and E. Witten, Nucl. Phys. B **460**, 506 (1996) [arXiv:hep-th/9510209].
- [48] P. Horava and E. Witten, Nucl. Phys. B **475**, 94 (1996) [arXiv:hep-th/9603142].
- [49] F. Lucchin and S. Matarrese, Phys. Rev. D **32**, 1316 (1985).
- [50] E. Witten, Nucl. Phys. B **471**, 135 (1996) [arXiv:hep-th/9602070].
- [51] G. Curio and A. Krause, Nucl. Phys. B **602**, 172 (2001) [arXiv:hep-th/0012152].
- [52] G. Curio and A. Krause, Nucl. Phys. B **693**, 195 (2004) [arXiv:hep-th/0308202].
- [53] E. Witten, Nucl. Phys. B **460**, 541 (1996) [arXiv:hep-th/9511030].
- [54] B. A. Ovrut, T. Pantev and J. Park, JHEP **0005**, 045 (2000) [arXiv:hep-th/0001133].
- [55] E. Buchbinder, R. Donagi and B. A. Ovrut, JHEP **0206**, 054 (2002) [arXiv:hep-th/0202084].

- [56] O. J. Ganor and A. Hanany, Nucl. Phys. B **474**, 122 (1996) [arXiv:hep-th/9602120].
- [57] N. Seiberg and E. Witten, Nucl. Phys. B **471**, 121 (1996) [arXiv:hep-th/9603003].
- [58] E. J. Copeland, A. R. Liddle and D. Wands, Phys. Rev. D **57**, 4686 (1998) [arXiv:gr-qc/9711068].
- [59] C. P. Burgess, R. Easther, A. Mazumdar, D. F. Mota and T. Multamaki, JHEP **0505**, 067 (2005) [arXiv:hep-th/0501125].
- [60] J. A. Adams, B. Cresswell and R. Easther, Phys. Rev. D **64**, 123514 (2001) [arXiv:astro-ph/0102236].
- [61] A. A. Starobinsky and J. Yokoyama, arXiv:gr-qc/9502002.
- [62] J. E. Lidsey, A. R. Liddle, E. W. Kolb, E. J. Copeland, T. Barreiro and M. Abney, Rev. Mod. Phys. **69**, 373 (1997) [arXiv:astro-ph/9508078].